LOW-RANK PHYSICAL MODEL RECOVERY FROM LOW-RANK SIGNAL APPROXIMATION

Charles Ethan Hayes, James H. McClellan, and Waymond R. Scott, Jr.

Georgia Institute of Technology
School of Electrical and Computer Engineering
Atlanta, GA, USA 30332-0250

ABSTRACT

This work presents a mathematical approach for recovering a physical model from a low-rank approximation of measured data obtained via the singular value decomposition (SVD). The general form of a low-rank physical model of the data is often known, so the presented approach learns the proper rotation and scaling matrices from the singular vectors and singular values of the SVD in order to recover the low-rank physical model of the data from the SVD approximation. By recovering the low-rank physical model, it becomes possible to exploit specific knowledge of the model to extract meaningful information for the physical application being studied. This work is useful for processing wide-band electromagnetic induction data—the motivating application.

Index Terms— low-rank model, SVD, ℓ_1-SVD, electromagnetic induction

1. INTRODUCTION

This work focuses on a mathematical derivation for recovering a low-rank model of a signal. The singular value decomposition (SVD) is a well known mathematical tool for obtaining a low-rank approximation from measured data. The SVD is a powerful tool and has been proven to be the optimal approximation of a low-rank matrix [1]. However, the SVD rarely has the same constraints as the low-rank model that is described through the physical properties of an application. This work builds upon the SVD by exploring the mathematical operations necessary to recover a low-rank physical model from the SVD. In a measurement system the low-rank physical model makes it easy to extract information about parameters that relate directly to properties described by equations, e.g., from acoustics or electromagetics.

This work is supported in part by the U.S. Army REDCOM CERDEC Night Vision and Electronic Sensors Directorate, Science and Technology Division, Countermine Branch and in part by the U. S. Army Research Office under Contract Number W911NF-11-1-0153.

2. BACKGROUND

The goal of this effort has been to improve the signal processing of wideband electromagnetic induction (WEMI) sensors. WEMI sensors are used for locating and classifying buried objects by energizing eddy currents within a conductive object and measuring the secondary magnetic fields as the object releases the energy. The object response is described by (o) independent tensors that govern the coupling of the sensors magnetic fields to the eddy currents and (r) exponential decay rates that govern the rate of energy release. These tensors and decay rates are physical properties of the object that can be used to classify the object.

WEMI sensors operate in a synthetic aperture mode by taking m (frequency response) measurements at n positions as the sensor passes over an object. The spatial response of the sensor is due to the sensor's magnetic fields, the object location, and the tensors, while the frequency response is due to the exponential decay rates and the tensors. With a detailed physical model that properly accounts for the tensors, it is possible to extract object location, exponential decay rates and tensors (the orientation of the object is embedded in the recovered tensor) with processing. The tensors are 3×3, positive semidefinite, and symmetric; and in the model, they are each expressed by a *tensor amplitude* written as a vector involving at most $p = 6$ parameters.

Previously, WEMI data has been processed in three stages: First, downtrack filtering that combines multiple location measurements to improve the signature strength [2, 3, 4]; second, recovery of the object's signature, by using the Discrete Spectrum of Relaxation Frequencies (DSRF) inversion [5, 6]; third, locating the object and determining its tensors by examining each DSRF frequency separately and using the tensor WEMI model [7].

Our most recent work with WEMI sensors creates a "filterless" processing scheme [4] by exploiting the dipole model [8, 9] for the target along with a reciprocity relationship [9, 10] to write the noise-free model in a form that is a product of a frequency and spatial response:

$$\hat{\mathbf{S}} = \mathbf{F}\,\mathbf{G}\,\mathbf{H}^T \tag{1}$$

where $\hat{\mathbf{S}} \in \Re^{m \times n}$ is the signal received from the object, $\mathbf{F} \in \Re^{m \times o}$ contains the object's frequency signatures, $\mathbf{G} \in \Re^{o \times p}$ contains the tensors that describe the object's coupling, and $\mathbf{H}^T \in \Re^{p \times n}$ contains the sensor's magnetic fields for a range of sensor positions that are used to sense the object and obtain its location. As for the dimensions, $p = 6$ and $o \leq 6$ are known from the model, $m = 42$ for the Georgia Tech WEMI platform, and n is roughly 100 depending on the number of location samples. Because $\min(o, p) \ll \min(m, n)$, a low-rank matrix is appropriate. The low-rank matrix approximation is obtained from the data by using the SVD. The desire to recover the physical model over the SVD representation is due to the fact that $\mathbf{G}$ has further unique properties that can be exploited, such as each row of $\mathbf{G}$ is a *tensor amplitude* representing a 3×3, positive semidefinite, and symmetric tensor. By recovering the physical low-rank model, it will be possible to implement further processing to exploit such knowledge.

It should be noted that the recent approach for WEMI sensors has clear similarities to the ℓ_1-SVD algorithm developed by Malioutov et. al. [11] for the direction of arrival (DOA) estimation problem. The DOA ℓ_1-SVD algorithm uses a model that can be described as $\mathbf{F}\,\mathbf{H}$, where $\mathbf{G}$ is the identity matrix. The SVD is used to create a low rank approximation, and a second order cone (SOC) optimization problem is created to extract the DOA information from the SVD. This connection implies that this new work could prove useful to a wider audience where the ℓ_1-SVD algorithm is of interest, but the application has a further desire to recover the entire low-rank model. Because of this potential generality, the remainder of this work is carried out in a general format for easy transference to other applications.

3. MODEL RECOVERY

The general model for noisy measurements

$$\mathbf{S} = \hat{\mathbf{S}} + \mathcal{E} = \mathbf{F}\,\mathbf{G}\,\mathbf{H}^T + \mathcal{E} \tag{2}$$

where $\hat{\mathbf{S}}$, $\mathbf{F}$, $\mathbf{G}$, and $\mathbf{H}$ are defined in (1), and $\mathcal{E}$ is a matrix of i.i.d. Gaussian noise. In order for the recovery to work, the model must span the smallest row and column subspaces possible. This is done by ensuring that $\mathbf{F}$ and $\mathbf{H}$ are full-rank matrices. In order to process the data, the SVD of $\mathbf{S}$ is taken to both recover a low-rank approximation and also denoise the signal. The SVD operation creates

$$\mathbf{S} = \mathbf{U_S}\,\mathbf{\Sigma_S}\,\mathbf{V_S}^T\,. \tag{3}$$

The SVD can be chosen to correctly approximate the low-rank matrix, but it enforces properties on the created matrices that are usually undesirable in the model, such as $\mathbf{\Sigma_S}$ is diagonal and $\mathbf{U_S}$ and $\mathbf{V_S}$ are both orthonormal. This work focuses on using the available information from the SVD to recover the original low-rank model from the data. The recovery of the low-rank model is accomplished by noting that

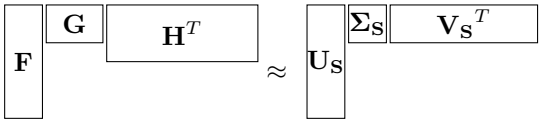

(4)

are equal except for the noise term (assumed small) that can be associated with the small singular values of the SVD.

Initially, we assume $o = p$ in (4), so $\mathbf{G}$ is square and the matrix pairs $(\mathbf{F}, \mathbf{U_S})$, $(\mathbf{G}, \mathbf{\Sigma_S})$, and $(\mathbf{H}, \mathbf{V_S})$ have the same dimensions. In the next section, a minor alteration will be introduced to relax this constraint.

3.1. Aligning subspaces

To simplify the discussion of recovering the low-rank model, it is useful to assume that $\mathbf{F}$ and $\mathbf{H}$ are known a priori, even though this assumption is unexpected in practice. Based on the relationship in (4), $\mathbf{F}$ and $\mathbf{U_S}$ span the same subspace, so

$$\mathbf{U_S} = \mathbf{F}\,\mathbf{Q}_U \tag{5}$$

where $\mathbf{Q}_U$ is a matrix responsible for orthogonalizing the columns of $\mathbf{F}$ and then unit scaling them. Because (4) is approximate when the measured data is noisy and $\mathbf{U_S} + \epsilon = \mathbf{F}\,\mathbf{Q}_U$ where ϵ is a noise term, it is necessary to solve (5) via

$$\min_{\mathbf{Q}_U} \| \mathbf{U_S} - \mathbf{F}\,\mathbf{Q}_U \|_2 \tag{6}$$

which leads to a standard least-squares solution

$$\mathbf{Q}_U = \mathbf{F}^\dagger\,\mathbf{U_S}, \tag{7}$$

where $\mathbf{F}^\dagger$ is the pseudo-inverse that is defined as $\mathbf{F}^\dagger = (\mathbf{F}^T\,\mathbf{F})^{-1}\,\mathbf{F}^T$. Just like $\mathbf{F}$ and $\mathbf{U_S}$, $\mathbf{H}$ and $\mathbf{V_S}$ span the same subspace, so the above discussion applies for getting $\mathbf{Q}_V \in \Re^{p \times p}$ via the least-squares minimization of

$$\min_{\mathbf{Q}_V} \| \mathbf{V_S} - \mathbf{H}\,\mathbf{Q}_V \|_2 \tag{8a}$$

$$\mathbf{Q}_V = \mathbf{H}^\dagger\,\mathbf{V_S}\,. \tag{8b}$$

3.2. Recovering the center term

Once the least squares solution for the subspaces are found, it is possible to recover $\mathbf{G}$. This is accomplished by inserting the relationships from (5) into (4) to obtain

$$\mathbf{U_S}\,\mathbf{\Sigma_S}\,\mathbf{V_S}^T = \mathbf{F}\,\mathbf{Q}_U\,\mathbf{\Sigma_S}\,\mathbf{Q}_V^T\,\mathbf{H}^T = \mathbf{F}\,\mathbf{G}\,\mathbf{H}^T \tag{9}$$

From (9) it becomes possible to recover $\mathbf{G}$ as

$$\mathbf{G} = \mathbf{Q}_U\,\mathbf{\Sigma_S}\,\mathbf{Q}_V^T. \tag{10}$$

With pseudo-inverses of $\mathbf{F}$ and $\mathbf{H}$, (10) can be rewritten as

$$\mathbf{G} = \mathbf{F}^\dagger\,\mathrm{U_S}\,\mathbf{\Sigma_S}\,\mathrm{V_S}^T\,\mathbf{H}^{\dagger T} = (\mathbf{F}^\dagger\,\mathbf{F})\,\mathbf{G}(\mathbf{H}^\dagger\,\mathbf{H})^T \tag{11}$$

3.3. Relaxing the model

In order to extend the model recovery method to the case where $o \neq p$, we must reexamine (10) when $\mathbf{G}$ is not square. The following discussion assumes $o < p$, which is the WEMI model, but a similar process can be applied if $o > p$. When $o < p$, the SVD produces ${\mathbf{V_S}}^T \in \Re^{o \times n}$ and $\mathbf{\Sigma_S} \in \Re^{o \times o}$, but $\mathbf{H}^T \in \Re^{p \times n}$. To relate $\mathbf{H}$ and $\mathbf{V_S}$ we propose

$$\mathbf{V_S} = \mathbf{H}\,\mathbf{B} \tag{12}$$

where $\mathbf{B} \in \Re^{p \times o}$ is not square. The same derivation as in (8a) and (8b) leads to the least-squares problem statement and solution for $\mathbf{B}$

$$\min_{\mathbf{B}} \| \mathbf{V_S} - \mathbf{H}\,\mathbf{B} \|_2 \tag{13a}$$

$$\mathbf{B} = \mathbf{H}^{\dagger}\,\mathbf{V_S}\,. \tag{13b}$$

Thus the matrix $\mathbf{B}$ replaces $\mathbf{Q}_V$ in (8a), so we recover $\mathbf{G}$ by rewriting (10) as

$$\mathbf{G} = \mathbf{Q}_U\,\mathbf{\Sigma_S}\,\mathbf{B}^T\,. \tag{14}$$

This result is the correct extension, but it should be noted that when $o \neq p$ the matrix $\mathbf{B}$ is not invertible. When $o > p$ the derivation is similar, but the square matrix $\mathbf{Q}_U$ in (10) would be replaced with a rectangular $o \times p$ matrix.

4. OBTAINING MODEL SUBSPACES

In order to obtain the low-rank model from the data, it was previously assumed that $\mathbf{F}$ and $\mathbf{H}$ were known a priori. In reality, obtaining valid matrices for $\mathbf{F}$ and $\mathbf{H}$ is the important problem of interest for recovering the model in (1). The solutions for $\mathbf{F}$ and $\mathbf{H}$ might be different and can be application specific. The benefit of recovering the low-rank model from the SVD is that it has completely decoupled the estimation of $\mathbf{F}$ and $\mathbf{H}$. The only joint estimation required occurs when obtaining $\mathbf{G}$. Separating these estimation problems better aligns with the model and allows for a more robust processing design. With respect to the WEMI application, this new approach should allow for a more accurate location estimation (from $\mathbf{H}$) than the three stage approach because the DSRF inversion errors (in $\mathbf{F}$) will no longer affect the location estimation. This work will introduce the two methods of interest for the WEMI application, as well as a third method that is obtained from the model relaxation section above. These methods are generic approaches to the solution that can serve as baseline approaches for choosing the matrices $\mathbf{F}$ and $\mathbf{H}$.

4.1. Subspace selection approach

The subspace selection (SS) approach is the first subspace matrix approach. SS is used when multiple options can be created from a model, but only a single option can be accurate. An example of this scenario is the position matrix $\mathbf{H}$ for the WEMI application. Using equations from the physical model, it is possible to simulate what $\mathbf{H}$ should be for any target location below the WEMI sensor. By creating a discrete grid of locations and simulating $\mathbf{H}$ for each of the grid points, it is possible to generate a large dictionary of $\mathbf{H}$'s. Under the assumption that the WEMI targets are physically separated such that the WEMI sensor is only interacting with one target at a time, obtaining the correct $\mathbf{H}$ becomes a problem of selecting the best $\mathbf{H}$ from the dictionary.

In order to select the best fitting $\mathbf{H}$, it is possible to use the relationships described in the model recovery. For the $p = o$ case, (8a) can be used as a measure of how well $\mathbf{H}$ fits the measured data. SS solves

$$\min_i \min_{\mathbf{Q}_V} \| \mathbf{V_S} - \mathbf{H}_i\,\mathbf{Q}_V^i \|_2 \tag{15}$$

where $\mathbf{H}_i$ is one entry in the dictionary of all possible $\mathbf{H}$'s. In words, (15) fits $\mathbf{V_S}$ from the SVD in (3) to all possible $\mathbf{H}$, and then selects the $\mathbf{H}_i$ that best aligns with the $\mathbf{V_S}$ subspace.

4.2. Sparse subspace creation approach

The sparse subspace creation (SSC) approach is the second subspace matrix approach. SSC is used when a sparse optimization problem can be designed to represent one of the subspaces. An example of this approach for the WEMI application would be using the DSRF to estimate the target's signature response $\mathbf{F}$. The DSRF allows $\mathbf{F}$ to be modeled as

$$\mathbf{F} = \mathbf{A}\,\mathbf{W} \tag{16}$$

where $\mathbf{A} \in \Re^{m \times z}$ is an over-complete dictionary, i.e., $z > m$, and $\mathbf{W} \in \Re^{z \times o}$ is a matrix of weights that select a few of the dictionary (column) vectors from $\mathbf{A}$ to create $\mathbf{F}$. The matrix $\mathbf{W}$ is sparse because most of the rows are zero. The matrix $\mathbf{A}$ is known from the physics of the WEMI sensor. The model of (16) can be inserted into (5) to obtain

$$\mathbf{U_S} = \mathbf{A}\,\mathbf{W}\,\mathbf{Q}_U = \mathbf{A}\,\mathbf{C} \tag{17}$$

where $\mathbf{C} = \mathbf{W}\,\mathbf{Q}_U$. The form of (17) is the same as the model used in [11] to derive the SOC optimization problem

$$\min_{\mathbf{C}} \| \mathbf{U_S} - \mathbf{A}\,\mathbf{C} \|_F^2 + \lambda \| \mathbf{C}^{\ell_2} \|_1 \tag{18}$$

where $\|.\|_F$ is the Frobenius norm, λ is a tuning parameter, and $\mathbf{C}^{\ell_2}$ is a vector containing the ℓ_2 norm of each row in $\mathbf{C}$. Other algorithms such as IAA [12] and M-FOCUSS [13] are also designed to solve problems such as (17).

It should be noted that SSC solves for $\mathbf{C}$ instead of $\mathbf{Q}_U$. Solving for the center of the model again as was done in (9) and (10) obtains

$$\mathbf{U_S}\,\mathbf{\Sigma_S}\,{\mathbf{V_S}}^T = \mathbf{A}\,\mathbf{C}\,\mathbf{\Sigma_S}\,\mathbf{Q}_V^T\,\mathbf{H}^T = \mathbf{A}\,\mathbf{W}\,\mathbf{G}\,\mathbf{H}^T \tag{19a}$$

$$\mathbf{W}\,\mathbf{G} = \mathbf{C}\,\mathbf{\Sigma_S}\,\mathbf{Q}_V^T \tag{19b}$$

for the SSC approach. For the WEMI application, the solution of $\mathbf{W}\,\mathbf{G}$ is of more interest than $\mathbf{G}$ alone. This is because $\mathbf{W}\,\mathbf{G}$ is the orientation tensor of a target that has been decomposed into a set of orthogonal basis vectors, $\mathbf{G}$, and their associated weights, $\mathbf{W}$.

4.3. Subspace projection approach

The subspace projection (SP) approach is the final subspace matrix approach. SP can be used when the model subspace is created from an unknown linear combination of a larger subspace. Start with the general model of $\mathbf{S} = \mathbf{F}\,\mathbf{G}\,\mathbf{H}^T$ and replace $\mathbf{H}$ with a linear combination of a larger (known) subspace that can be written as

$$\mathbf{H} = \mathbf{Y}\,\mathbf{Z} \tag{20}$$

where $\mathbf{Y} \in \Re^{n\times w}$, $\mathbf{Z} \in \Re^{w\times p}$, and $w > p$. Then we write

$$\mathbf{S} = \mathbf{F}\,\mathbf{G}\,\mathbf{H}^T = \mathbf{F}(\mathbf{G}\,\mathbf{Z}^T)\,\mathbf{Y}^T = \mathbf{F}(\mathbf{G}_Z^T)\,\mathbf{Y}^T \tag{21}$$

By using (13b) with $\mathbf{Y}$ replacing $\mathbf{H}$ we obtain

$$\mathbf{B}_Y = \mathbf{Y}^\dagger\,\mathbf{V}_\mathbf{S}\,. \tag{22}$$

Then repeating (14) for the new model, we get

$$\mathbf{G}\,\mathbf{Z}^T = \mathbf{G}_Z = \mathbf{Q}_U\,\mathbf{\Sigma}_\mathbf{S}\,\mathbf{B}_Y^T\,. \tag{23}$$

which shows that $\mathbf{G}\,\mathbf{Z}^T$ can be recovered when $\mathbf{Y}$ is known.

5. RESULTS

In order to confirm the low-rank physical model recovery proposed, simulations were run for the WEMI application. A target with three metal loops was simulated, where each loop contains a unique exponential decay rate and the loop tensors are orthogonal. The simulations also used 600 positions which creates a signal model having $m = 42$, $o = 3$, $p = 6$, and $n = 600$. Each run simulated a random exponential decay rate for the loops and the target was rotated in a random direction. The signal to noise ratio (SNR) has been defined as the ratio between the smallest singular value of $\hat{\mathbf{S}}$ and the largest singular value of $\mathcal{E}$ where $\mathcal{E} \in \Re^{42\times 600}$ is the noise matrix that is populated from an i.i.d. $\mathcal{N}(0,1)$ distribution. Multiple SNRs are examined in Fig. 1, where the average error from 100 runs is presented for each SNR. The error has been calculated as $\frac{\|\,\mathbf{G}-\hat{\mathbf{G}}\|_F}{\|\hat{\mathbf{G}}\|_F}$, where $\|.\|_F$ is the Frobenius norm and $\hat{\mathbf{G}}$ is the estimated $\mathbf{G}$ from the simulated data.

As seen in Fig. 1, recovering the tensor information $\mathbf{G}$ with the known subspace problem is very accurate. The SS approach exhibits equivalent performance, indicating that (15) can accurately select $\mathbf{H}$. The SP approach is slightly worse, as some error is incurred from the least-squares approximation of the smaller subspace. SSC is comparable to SS for high SNRs, but SSC struggles to find the correct basis at lower SNR values which leads to large errors. In fact, the Frobenius error is a poor metric for SSC because it reports a large error when SSC chooses a reordering of the correct basis. The median is displayed to remove these outliers.

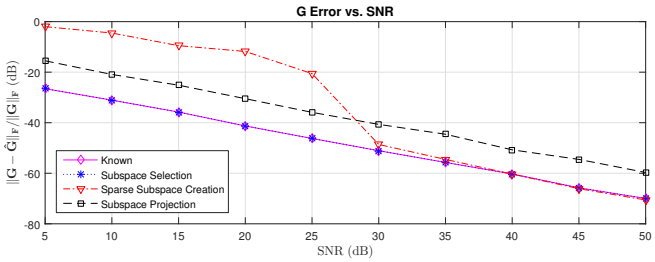

Fig. 1. The error vs. SNR curve for recovering $\mathbf{G}$ from simulated WEMI data using the proposed methods.

This low-rank physical model recovery technique has also been applied successfully to laboratory data and WEMI field measurements. The results are very encouraging for the recovery of tensor information which is the most challenging task. Due to space limitations these processing results are not included here, but have been submitted for publication [14].

6. CONCLUSION

This work has presented a method for recovering the low-rank physical model from the SVD low-rank approximation of the measured signal. This low-rank model recovery has been accomplished by recognizing that the $\mathbf{U}_\mathbf{S}$ and $\mathbf{V}_\mathbf{S}$ from the SVD have to span the same subspace as the matrices in the model. By fitting a rotation and scaling matrix for each of these subspaces, it is possible to recover the physical model from the SVD. This work showed how the physical model could be recovered when the middle matrix in the physical model is both square and rectangular. The recovery process has been presented in a generic format, where the only application specific portion originates from subspaces that the equations of the physical model define. Three possible approaches for finding the subspaces were presented which should cover a wide variety of applications.

The discussed model recovery technique is designed to transform a low-rank approximation from data into a physical model. This recovery should be performed when there is further knowledge about the physical model that can be exploited beyond the low-rank nature. This specific work has been designed for Wideband Electromagnetic Induction (WEMI) processing. Figure 1 demonstrated the effectiveness of the low rank model recovery method on simulated WEMI data. The $\mathbf{G}$ for the WEMI data was accurately recovered, which will allow further processing to exploit the known structure of $\mathbf{G}$ from the physical model.

7. REFERENCES

[1] C. Eckart and G. Young, "The approximation of one matrix by another of lower rank," *Psychometrika*, vol. 1, no. 3, pp. 211–218, 1936.

[2] C. Bruschini, *A Multidisciplinary Analysis of Frequency Domain Metal Detectors for Humanitarian Demining*, Ph.D. thesis, Vrije Universiteit Brussel, 2002.

[3] Mu-Hsin Wei, W.R. Scott, Jr., and J.H. McClellan, "Adaptive prefiltering for nonnegative discrete spectrum of relaxations," *IEEE Geoscience and Remote Sensing Letters*, vol. 12, no. 5, pp. 1018–1022, May 2015.

[4] C.E. Hayes, J.H. McClellan, W.R. Scott, Jr., and A.J. Kerr, "Improved electromagnetic induction processing with novel adaptive matched filter and matched subspace detection," *Proc. SPIE*, vol. 9823, pp. 98230E–98230E–14, 2016.

[5] Mu-Hsin Wei, W.R. Scott, Jr., and J.H. McClellan, "Robust estimation of the discrete spectrum of relaxations for electromagnetic induction responses," *IEEE Trans. Geoscience and Remote Sensing*, vol. 48, no. 3, pp. 1169–1179, Mar. 2010.

[6] C.E. Hayes, J.H. McClellan, and W.R. Scott, Jr., "Sparse recovery using an SVD approach to interference removal and parameter estimation," in *2015 IEEE Signal Processing Workshop*, 2015, pp. 202–207.

[7] K.R. Krueger, W.R. Scott, Jr., and J.H. McClellan, "Location and orientation estimation of buried targets using electromagnetic induction sensors," *Proc. SPIE*, vol. 8357, pp. 83570D–83570D–12, 2012.

[8] C. E. Baum, "Detection and identification of mines from natural magnetic and electromagnetic resonances," in *Detection and identification of visually oscured targets, C. E. Baum, Ed., ed Philadelphia: Taylor and Francis*, 1999, pp. 163–218.

[9] G.D. Larson and W.R. Scott, Jr., "Modeling the measured EM induction response of targets as a sum of dipole terms each with a discrete relaxation frequency," in *2010 IEEE International Geoscience and Remote Sensing Symposium (IGARSS), Honolulu, HI*, 2010, pp. 4188–4191.

[10] H. Vesselle and R. E. Collin, "The signal-to-noise ratio of nuclear magnetic resonance surface coils and application to a lossy dielectric cylinder model. I. Theory," *IEEE Trans. Biomedical Engineering*, vol. 42, no. 1, pp. 497–506, Jan. 1995.

[11] D. Malioutov, M. Cetin, and A. S. Willsky, "A sparse signal reconstruction perspective for source localization with sensor arrays," *IEEE Trans. Signal Processing*, vol. 53, no. 8, pp. 3010–3022, Aug. 2005.

[12] T. Yardibi, J. Li, P. Stoica, M. Xue, and A.B Baggeroer, "Source localization and sensing: A nonparametric iterative adaptive approach based on weighted least squares," *IEEE Trans. Aerospace and Electronic Systems*, vol. 46, no. 1, pp. 425–443, Jan. 2010.

[13] S.F. Cotter, B.D. Rao, K. Engan, and K. Kreutz-Delgado, "Sparse solutions to linear inverse problems with multiple measurement vectors," *IEEE Trans. Signal Processing*, vol. 53, no. 7, pp. 2477–2488, July 2005.

[14] C.E. Hayes, J.H. McClellan, and W.R. Scott, Jr., "Novel model based EMI processing framework," *Proc. SPIE*, Apr. 2017, Accepted.